Characteristics of a Liquefied Butane Spray

J. Y. Koo*, H. C. Chung*, J. S. Shakal, and S. Goto****

(Received April 7, 1997)

The characteristics of a butane spray from pintle-type injector were studied by droplet velocity and diameter measurements and high-speed photography. The accumulator type injector operated off a common rail fuel supply system operated at 13 MPa, and was controlled by a high-speed solenoid valve. Injection was carried out in a chamber at ambient temperature and at the pressure above (0.37 MPa) and below (0.15 MPa) the fuel vapor pressure. Two-component phase/Doppler particle analyzer and traverser were used to obtain the droplet diameter and the velocity at numerous locations in the spray. The entire injection event was analyzed as a time-average and also subdivided into three temporal intervals, A, B, and C. The high-speed photographs showed a narrower cone angle during the quasi-steady spray period at the 0.37 MPa chamber pressure compared to the 0.15 MPa case.

Key Words: Liquefied Butane Spray, Sauter Mean Diameter(SMD), High Speed Photographs

1. Introduction

Recently the concern about an environmental protection and improvement of energy efficiency of the combustion system is more increasing. The use of "clean fuels" such as butane, propane, and mixtures of these (LPG) is an attractive way to reduce exhaust emissions(Sinor Consultants Inc., 1995). The advantage of usage of butane for an internal combustion engine is that it emitts small amount of soot owing to the smaller number of carbon compared to the conventional fuel.

Engine efficiency, however, can be limited by the compression ratio for homogeneous and lean-burn Otto-cycle engines due to knocking, because the fuel and air are both present during the compression stroke. Direct injection allows a higher compression ratio and more diesel-like thermal efficiency, which is important for heavy-duty applications such as trucks and buses. For this purpose, the fuel injection pressure does not have to be as high as in diesel engines (>50 MPa), but higher than in the typical gasoline Otto-cycle engines (about 0.5 MPa). Hence, a pintle type injector are chosen because a conical spray is obtained with no solid core region where droplet diameters are large and vaporization slow (Senda, 1992).

In Korea, many taxis are operating on LPG fuel. In foreign countries, Holland for example, there are currently about 2,100 LPG filling stations and 600,000 to 700,000 compact type cars with 2 to 3 liter LPG engines. This is equivalent to 10 to 12% of the total number of cars. In Vienna city, where public pollution is a primary concern, LPG has been used in local city buses since the sixties, and now about 500 LPG buses are in operation. In Japan there are about 320,000 vechiles, mainly taxis, operating on LPG fuel and about 2,000 filling stations concentrated in larger cities. Vehicular emissions regulations are being gradually tightened, however significantly more stringent regulations for large type diesel vehicles are planned to take effect in a few years, in addition to special restrictions covering large metropolitan areas. The infrastructure for vehicular LPG filling stations is gradually being put in

* Hankuk Aviation University, 200-1, Hwajeon-dong, Koyang-shi, Kyungki-do, 412-791, Korea
** AIST MITI Mechanical Engineering Laboratory, Namiki, Tsukuba, 305, Ibaraki, Japan

place, and the need for reduced emissions provides motivation for development of high-efficiency direct injection LPG engines for large heavy-duty vehicles.

2. Previous Research

There have been many studies done of the gasoline and diesel injection processes(Koo, 1994; Park, 1996) but very few of liquid-phase low-boiling point alternative fuels like butane, propane, or mixtures of these(Karim, 1988; Tanakka, et al., 1995). As part of a dual-fuel engine development effort, Goto (1992, 1993) compared hole-type and pintle-type injectors by injecting butane, propane, and auto gas (80% butane+20% propane) into ambient temperature and pressure air, and observing the spray with a high-speed camera and performing the image analysis. Laser Doppler Velocimetry (LDV) was also used to measure the transient spray velocity at several locations in the hole nozzle spray. The injectors were operated at 0.7 MPa injection pressure and, aside from the nozzle, resembled a typical solenoid actuated production automotive SI engine injector. Their results showed that the pintle nozzle was associated with more uniform atomization and quicker vaporization. The hole nozzle resulted in the spray pattern that resembled a column of liquid. The hole nozzle spray diffused more slowly into the ambient gas than the pintle nozzle spray. LDV measurements showed a maximum injection velocity of about 40 m/s. Unvaporized fuel particles were observed about 20 cm from the injector nozzle with a 5ms injection time, but with a 20 ms injection time unvaporized fuel was observed beyond 40 cm from the injector.

3. Experimental Apparatus

3.1 Injector, chamber, and measurement apparatus

A common rail accumulator type pintle injector (CR-G2 from BKM Inc.) as shown in Fig. 1 was used for this study. The fuel was supplied by a multi-piston pump with a 100 cc capacity accumulator to help the absorption of the pressure fluctuations caused by the injection process. With this type of injector, opening the solenoid

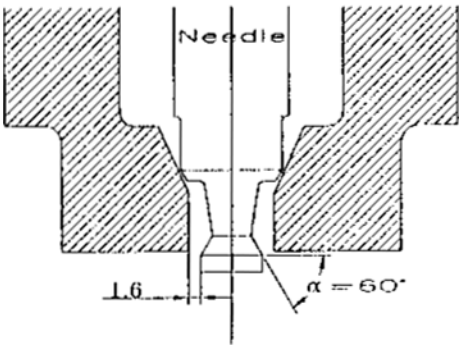

Fig. 1 Detail of pintle type butane nozzle.

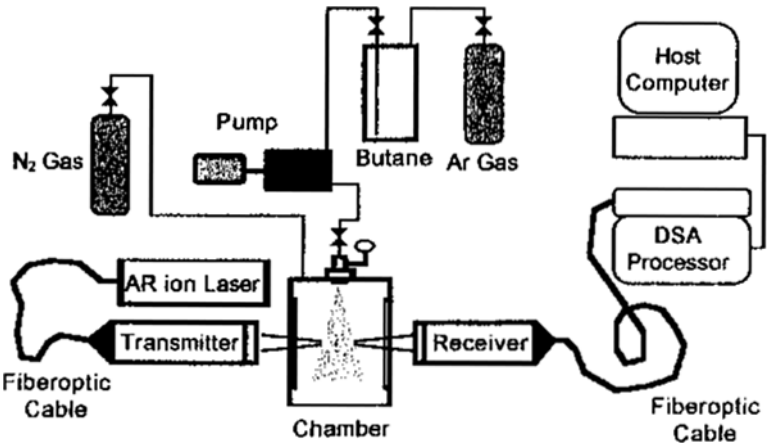

Fig. 2 PDPA spray measurement system.

valve created a pressure imbalance across the needle, which then rose to release the fuel contained in the accumulator. The injection duration was then controlled by the rail pressure, which was approximately the initial injection pressure. An external timing source provided the injector trigger and a 12 bit timing signal resulted in 11ms temporal resolution. The entire injection event was analyzed as a time-average and also subdivided into three temporal intervals, A, B, and C. Interval A generally corresponded to the actual time fuel was being injected, interval B to the period after injection had stopped and the spray cloud was passing through the measurement point, and interval C to the entrained flow. Figure 2 shows a schematic of the Phase/Doppler Particle Analyzer(PDPA) Measurement system. When injecting into ambient air, relatively large droplets (100μm) were detected after injection had ended. These did not appear when using nitrogen ambient gas, so it was presumed that water was condensing out of the air. Thus, nitrogen was used as purge gas, to carry away the injected fuel. A specially shaped manifold pipe was installed inside the chamber to evenly distribute the nitrogen and avoid creating an artificial ambient flow. The PDPA (Aerometrics DSA) was used with a 30 degree forward scatter collection angle and three-axis traverser unit (Unidex 11) to measure the droplet velocity and size at an array of 73 (0.15MPa chamber pressure case) and 35 (0.37MPa chamber pressure case) axial and radial positions. At least 2000 valid samples were obtained at each location and the laser power output was 2W. To avoid the problems of dense spray measurement, a 250 mm focal length transmitter lens was used. The fuel was butane, with main properties shown in Table 1. The injection

Table 1 Fuel properties.

Composition	n-butane
Density	0.581g/cm^3
Vapor Pressure(298K)	0.23 MPa
Refractive Index	1.355 at 15 deg. C
Viscosity	3.1×10^{-7} m^2/s

pressure was measured by a strain gauge type sensor (Kyowa PE-200 KWS) at the injector rail inlet. The pressure differential across the injector nozzle ($\triangle P_{inj}$) was measured by a strain gauge attached to the outside of the accumulator.

3.2 High-speed photography system

The same chamber, injector, fuel, and fuel supply system were used as in the PDPA measurements. Figure 3 shows the schematic of photographic system. A 35 W Copper Vapor Laser (Oxford Lasers, ACL-35) and 16 mm high-speed camera (nac E-10) were used to take the photographs, with the camera providing a trigger to the laser so that one frame contained one laser pulse. Images shown here were taken at 9090 frames per second. Kodak 7222 black and white film was

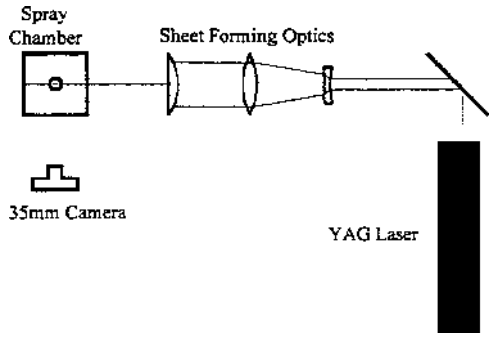

Fig. 3 Schematic of photography system.

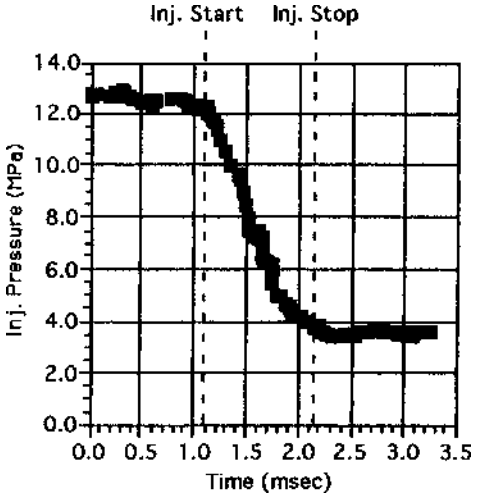

Fig. 4 Fuel injector pressure history as measured by a strain guage attached to the accumilator.

used. The laser sheet thickness was 0. 5 mm at the injector axis and the pulse duration was estimated at about 10 ns.

4. Results

4.1 Injection characteristics

Figure 4 shows the injection pressure profile. When the injection started, the pressure was 12. 5 MPa, and dropped to about 4MPa at the end of

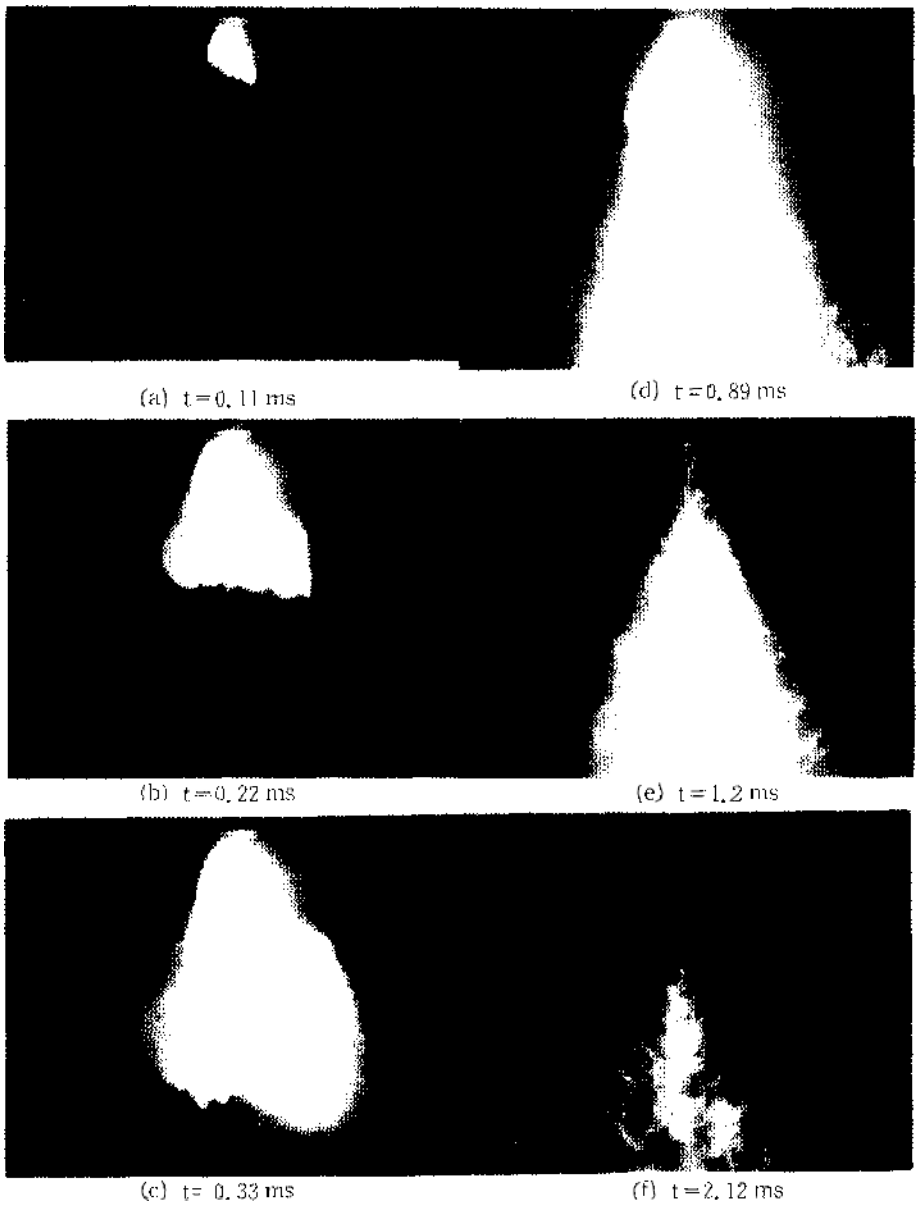

Fig. 5 High-speed photographs at 0.15 MPa chamber pressure (the elapsed time after injection start is shown below each figure).

injection, resulting in an injection duration of 1ms. A lower needle closing pressure was normally observed with this type of injector, but for these tests it was not adjusted.

4.2 Spray photographs

Photographs at chamber pressures of 0.15 MPa and 0.37 MPa are compared, as shown in Figs. 5 and 6, respectively. The time after injection start is shown below each image. The spray is not symmetric and in other pictures fuel are seen to emerge from the right side of the nozzle first. At 0.15 MPa chamber pressure, the first three image pairs yield tip penetration velocities of 38 m/s, 68 m/s, and 87 m/s. At 0.37 MPa chamber pressure the first two image pairs yield tip penetration

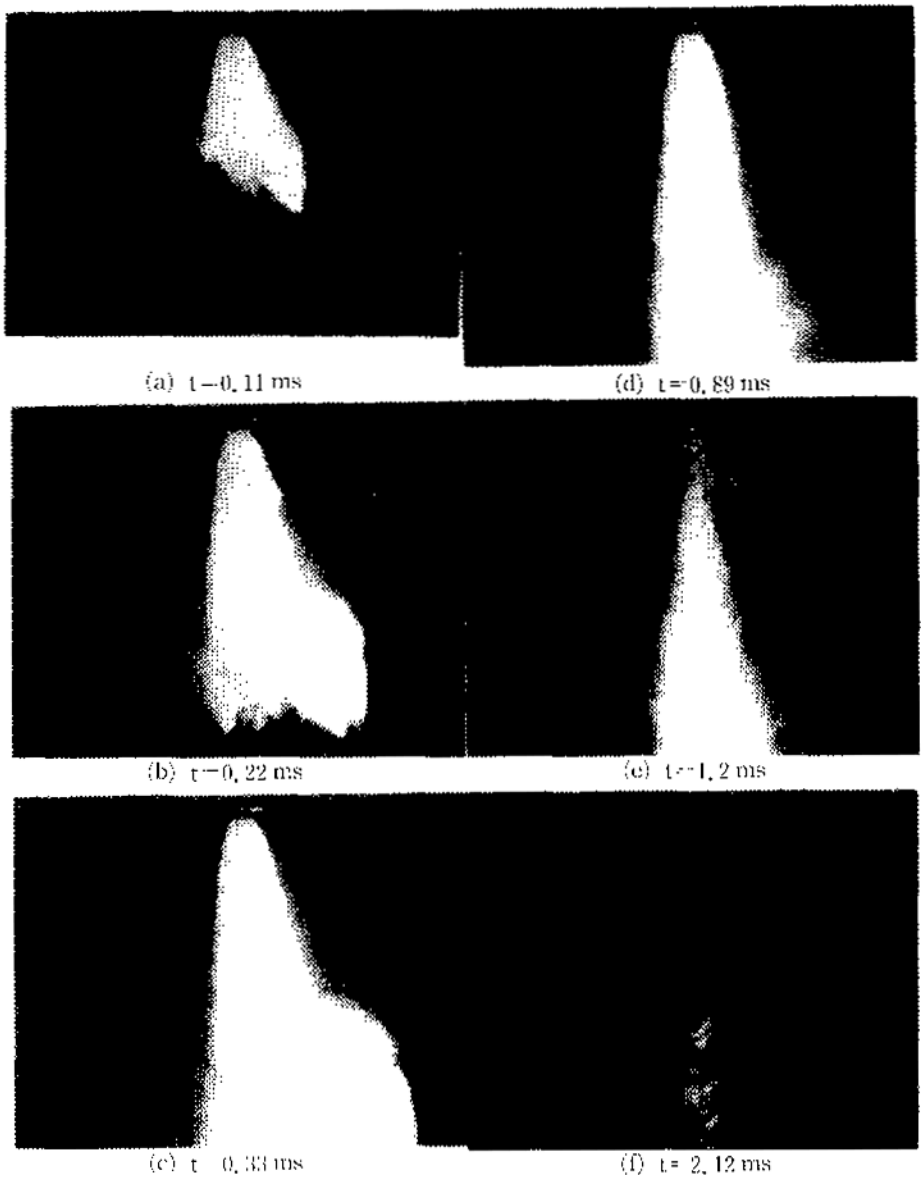

Fig. 6 High-speed photographs at 0.37 MPa chamber pressure (the elapsed time after injection start is shown below each figure).

velocities of 121 m/s and 87 m/s. Except at the leading edge, the spray is too dense for droplets or other features inside the spray to be identified. A large vortex forms at the leading edge of the spray cone within 0. 3 ms of injection start. The outer part of the vortex quickly loses momentum but the inner part is swept downstream by newly injected fuel, further concealing the actual spray structure. This was most apparent for the 0.15MPa chamber pressure case. The images at t =0.89 ms, during the quasi-steady portion of injection, show that the cone angle decreases from 37 degree to 22 degree when the chamber pressure was increased from 0.15 MPa to 0.37 MPa. After the injection stopped, the spray took on a fish -bone structure in the higher chamber pressure and a web-like structure in the ambient chamber pressure case. Image (f) in the lower right of Figs. 5 and 6 show the spray structure 2.1 ms and 1.8ms after injection start, respectively. At 0.37 MPa chamber pressure, the spray is decelerated but a higher ambient heat capacity is able to evaporate the fuel more rapidly even though this is above the fuel vapor pressure. It is theorized that due to rapid local cooling during injection, evaporation of the spray is slower at the 0.15 MPa chamber pressure, which is below the fuel vapor pressure. Secondary injections sometimes occurred and resulted in bursts of relatively large slow-moving droplets being injected into a relatively cold region.

4.3 Velocity and diameter data

In this study entire injection event was analyzed as a time-average and also subdivided into three temporal intervals, A, B, and C. Interval A generally corresponded to the actual time fuel was being injected, interval B to the period after injection had stopped and the spray cloud was passing through the measurement point, and interval C to entrained flow.

Looking first at the average velocity, shown in Fig. 7, it can be seen that the velocities near the injector are lower at 0.37 MPa chamber pressure, but further away from the injector there is not much difference. The evidence of entrainment is seen at the lower chamber pressure.

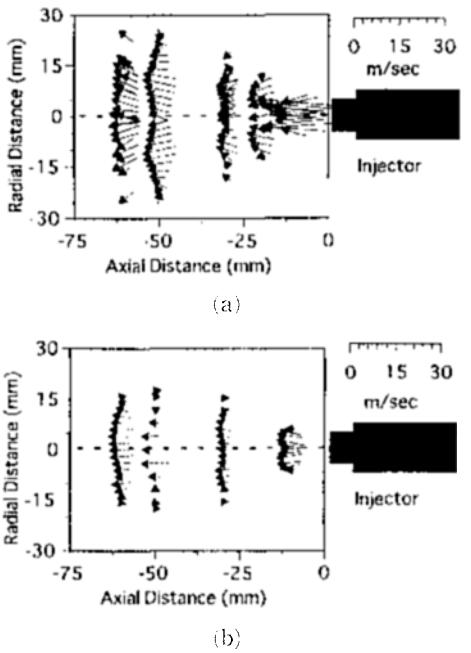

Fig. 7 Average particle velocity at 0.15 MPa chamber pressure (a) and 0.37 MPa chamber pressure (b).

Plots of Sauter mean diameter (SMD) are shown in Fig. 8 for 0.15 MPa and in Fig. 9 for 0.37 MPa chamber pressure. During interval A, the only remarkable feature at 0.15 MPa chamber pressure is a pair of small peaks near the axis at about 50 mm from the injector. At 0.37 MPa chamber pressure there is much wider variation in SMD in both axial and radial directions. Larger SMDs are seen near the injector and near the axis at about 50 mm from the injector. At the edges of the spray the SMDs are similar for both chamber pressures, e. g. 10 to 15μm. During interval B at 0.15 MPa chamber pressure, two peaks appear near the injector and the SMD reaches 20μm in these regions. Further away from the injector the SMD is centered at about 15μm. At 0.37 MPa chamber pressure there is again much wider variation in SMD, and values near the injector surpass 35μm. The SMD peaks seen at about 50 mm axial distance are much smaller in interval B and are nearly merged into one single peak. During interval C, the lower chamber pressure case shows two sharply higher peaks near the injector and gradu-

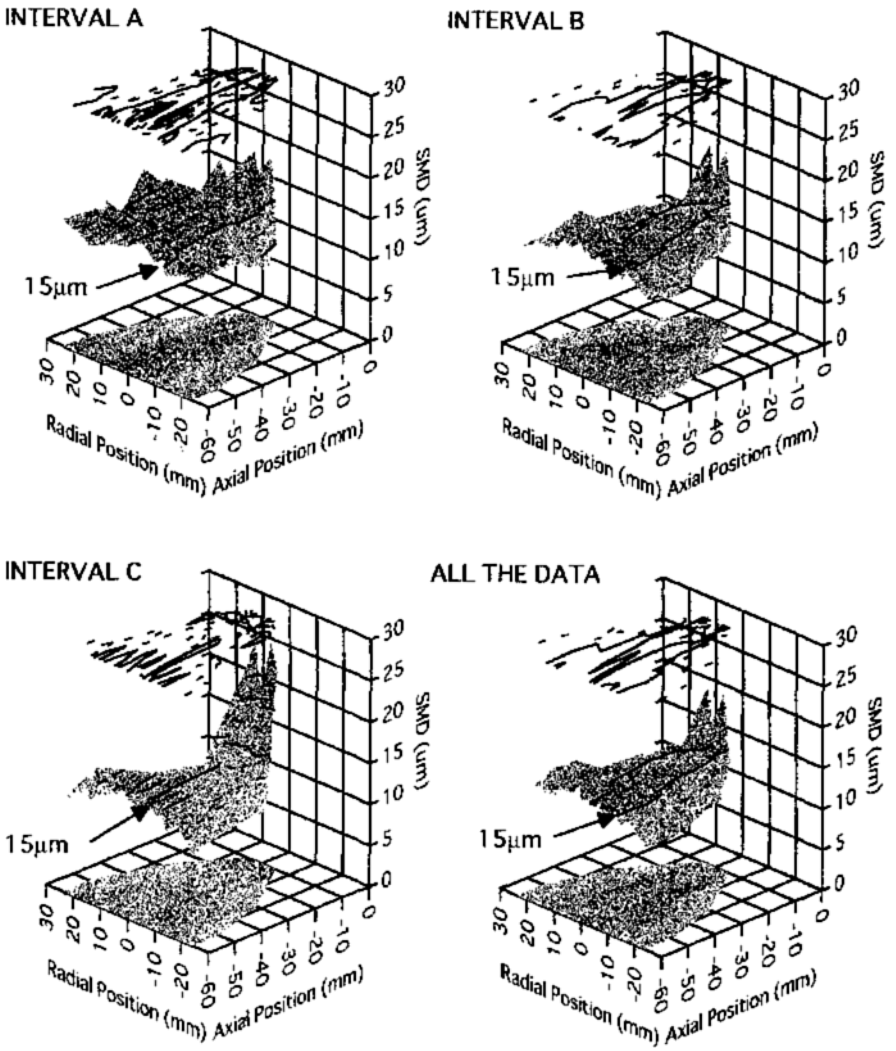

Fig. 8 Measured Droplet SMD for the 0.15 MPa chamber pressure case during the three time intervals (A, B, and C) and for all the data.

ally decresing SMD further away from the nozzle. The spray edges show similar SMD (10 to 13μm) during all three intervals. It is presumed that the SMD peaks near the injector are caused by secondary injection(s). At 0.37 MPa chamber pressure, intervals B and C are fairly similar. Overall, the lower chamber pressure case shows less spatial variation in SMD and about 5 to 7μm lower values at the spray edges. Also two peaks in SMD appear at 50 to 60 mm from the injector, whereas at 0.37 MPa chamber pressure there is only one peak there.

These results indicate that the spray structure depends on the ambient pressure, which in this comparison are below (0.15 MPa) and above (0.37 MPa) the fuel vapor pressure. Evidence of a conical spray is seen at the lower chamber pressure case, but at 0.37 MPa chamber pressure a conical spray may exist initially but it later changes to one more typical of a hole nozzle.

Figures 10 and 11 show the validation rate for 0.15 MPa and 0.37 MPa chamber pressure, respectively. As one may expect, the validation rate for both cases is very low during interval A due to the thick spray. Higher values are seen during interval B for both cases. Large spatial variation

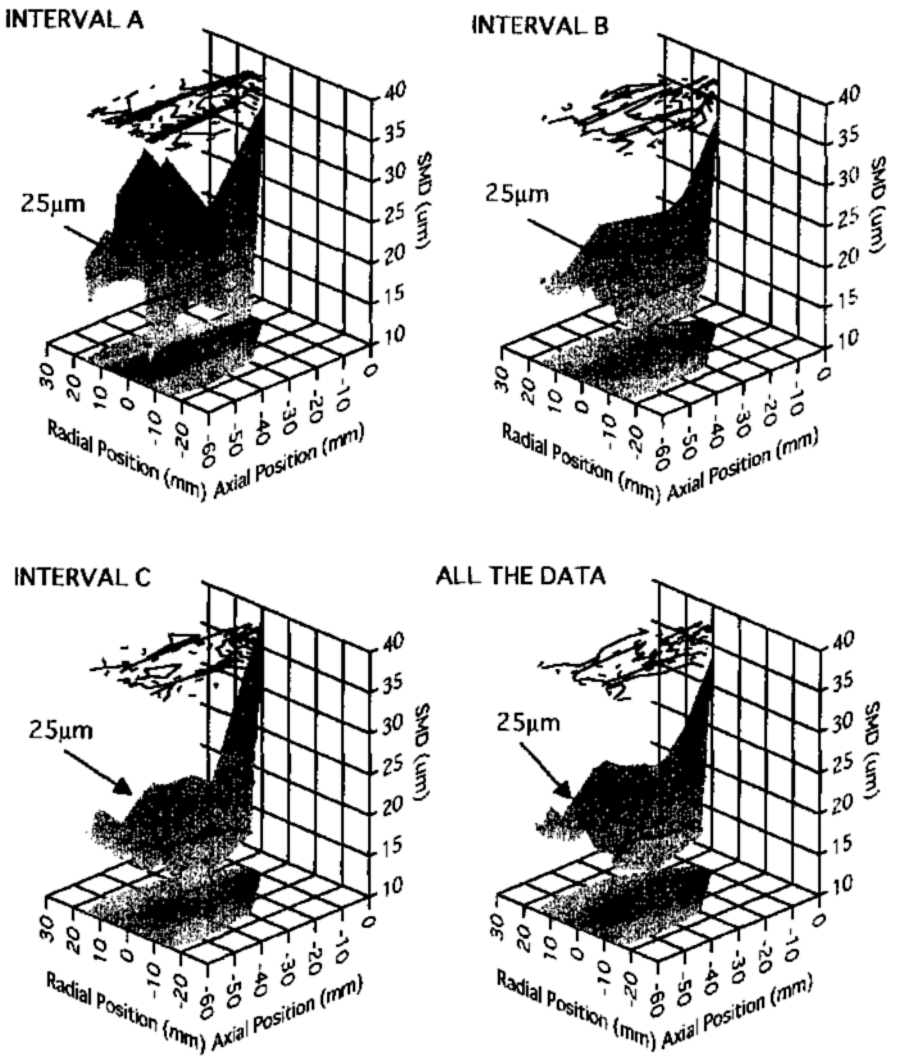

Fig. 9 Measured Droplet SMD for the 0.37 MPa chamber pressure case during the three time intervals (A, B, and C) and for all the data.

is seen during interval C, with higher validation rates appearing in the central and edge regions of the spray. Overall, at 0.15 MPa the validation rate drops off rapidly out to about 20 mm from the injector and then rises to about 65%. For the 0.37 MPa chamber pressure case the overall validation rate is more uniform centered at about 75%.

5. Summary

The high-speed photographs showed a narrower cone angle during the quasi-steady spray period at the 0.37 MPa chamber pressure compared to the 0.15 MPa chamber pressure. Except at the leading edge, during injection the spray was very dense and it was difficult to identify individual droplets or other features inside the spray. A vortex formed within 0.3 ms of the start of injection at the leading edge of the spray cone, and was most apparent for the 0.15 MPa chamber pressure case. After injection stopped however, a fish-bone structure appeared at the higher chamber pressure and a web-like structure appeared in the lower chamber pressure case. The spray appeared to evaporate faster at 0.37 MPa chamber pressure, even though this was above the fuel

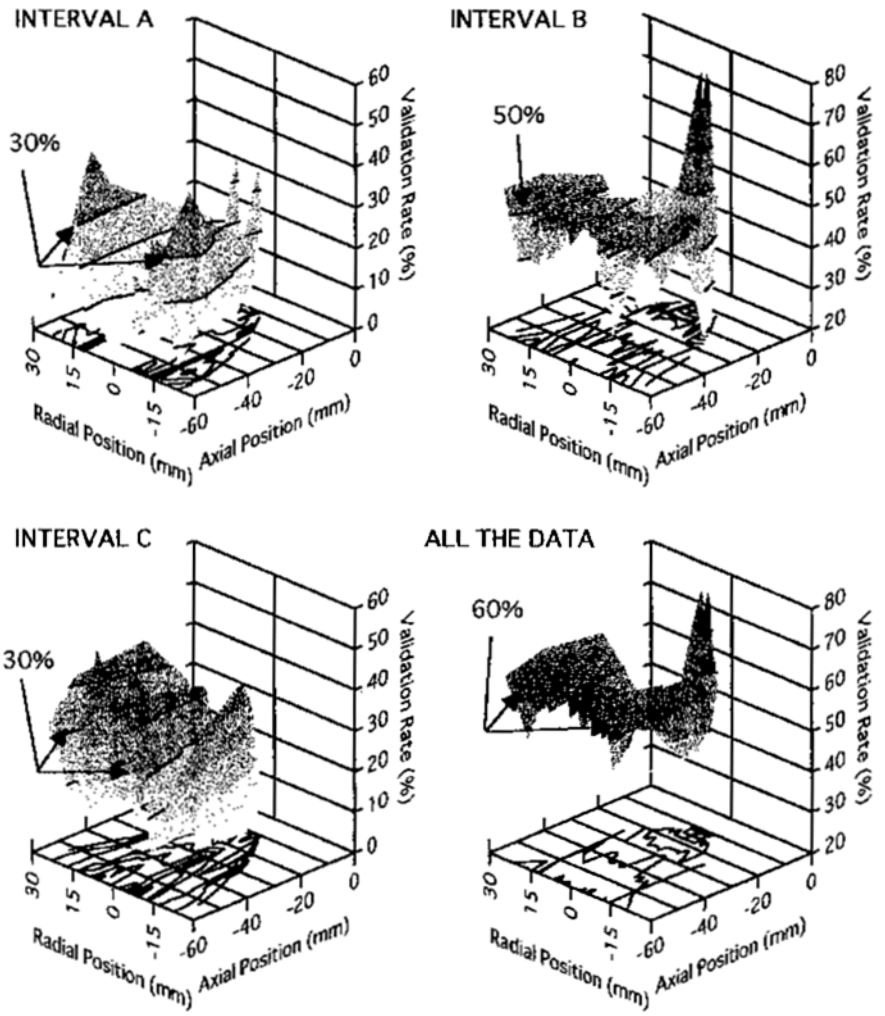

Fig. 10 Validation rate for the 0.15 MPa chamber pressure case during the three time intervals (A, B, and C) and for all the data.

vapor pressure.

Comparing the Sauter mean diameter (SMD) at 0.37 MPa and 0.15 MPa during interval A, much wider spatial variation was seen at the higher chamber pressure. SMDs were similar at the spray edges (10 to 15μm) but nearly double in the interior. During interval B the two peaks in SMD at 0.37 MPa chamber pressure began to merge and the spray structure resembled that of a hole nozzle during interval C and on the average over all three intervals. During interval C there appeared one (0.37 MPa chamber pressure) or two (0.15 MPa chamber pressure) sharp SMD peaks near the injector--these were thought to be due to secondary injections. Validation rates of interval A and parts of B and C were quite low for the 0.15 MPa chamber pressure case, which means generalized conclusions for these portions may not be sound. For the 0.37 MPa chamber pressure case the spray was not evaporating as rapidly and thus the validation rate was noticeably higher.

Acknowledgements

The authors appreciate the helpful advise and discussions of Mr. Y. Uchiyama. This study was supported by KOSEF Core Project #961-1005

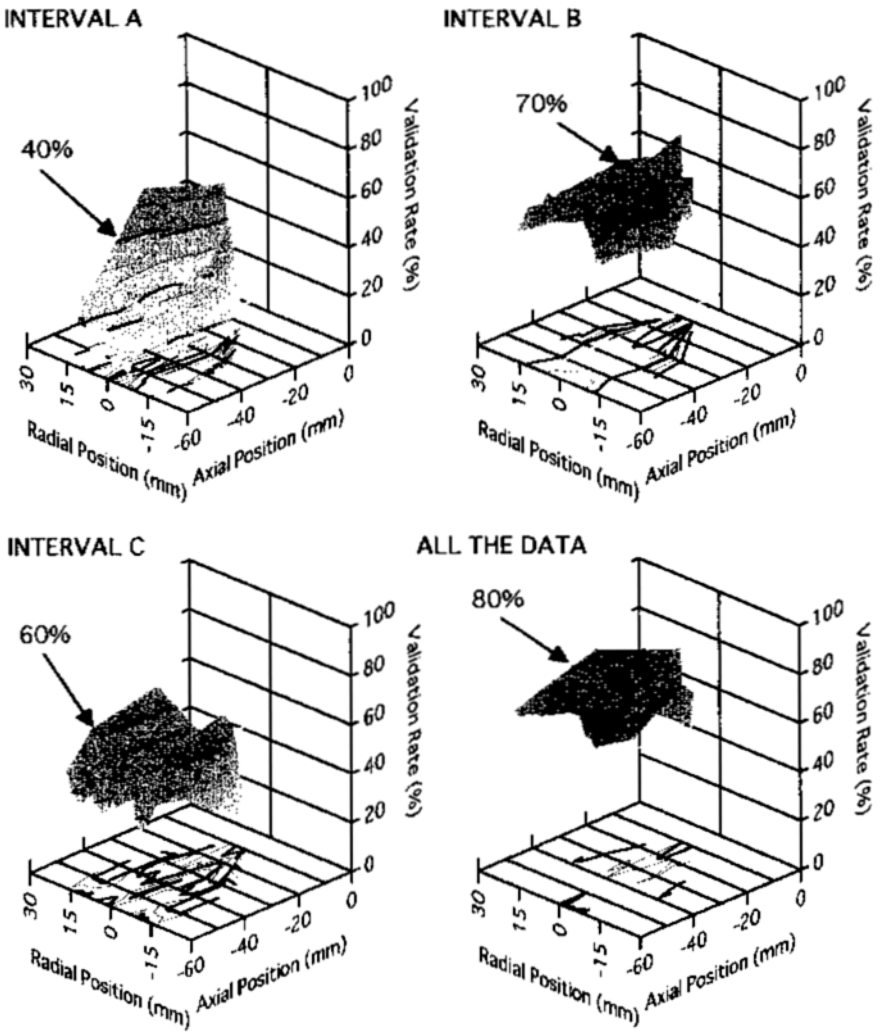

Fig. 11 Validation rate for the 0.37 MPa chamber pressure case during the three time intervals (A, B, and C) and for all the data.

-042-2.

References

Goto, S., Furutani, H., and Delic, R. D., 1992, "Dual-Fuel Diesel Engine Using Butane," *SAE Paper* 920690.

Goto, S., Furutani, H., Komori, M., and Yagi, M., 1993, LPG "Diesel Engine: Dual Fuel Method," *SAE Paper,* 9300747.

Karim, G. A. Zhaoda, Y., 1988, "An Analytical Model for Knock in Dual Fuel Engines of the Compression Ignition Type," *SAE Paper* 880151.

Koo, J. Y., 1994, "Phase Doppler Measurements and Probability Density Functions in Liquid Fuel Spray," *Transactions of the KSME,* Vol. 18, No. 4, pp. 1039~1049.

Park, K., 1996, "A Study on the Shaped Combustion System Using Diesel Spray Impinged on a Wall," *KSME Journal,* Vol. 10, No. 3, pp. 351~361.

Senda, J., Nishikori, T., Tsukamoto, T., and Fusimoto, H., 1992, "Atomization of Spray under Low-Pressure Field from Pintle Gasoline Injector," *SAE Paper* 920382.

Sinor Consultants Inc., 1995, *The Clean Fuels Report,* pp. 100~105.

Tanaka, D., Hojyo, Y., Senda, J., and Fujimoto, 1995, "Numerical Analysis of Flash Boiling Spray, *5th Symposium (ILASS-Japan) on Atomization,* pp. 252~257.